JETIR.ORG ISSN: 2349-5162 | ESTD Year : 2014 | Monthly Issue
JOURNAL OF EMERGING TECHNOLOGIES AND INNOVATIVE RESEARCH (JETIR)
An International Scholarly Open Access, Peer-reviewed, Refereed Journal

DESIGN AND ANALYSIS OF 5-LEVEL MLI FOR GRID INTEGRATION OF PPCS USING DIFFERENT MPPT TECHNIQUES

[1]Ananth Gowda R C, [2]Dr. Madhusudhana J.

[1]M Tech Student, [2]Associate Professor
[1]Department of Electrical Engineering,
[1]University Visvesvaraya College of Engineering, Bangalore, India

Abstract: The main objective of this work is to propose an improved H-Bridge multilevel inverter in the Photovoltaic power conversion system (PPCS) which is connected to the distributed grid. The power quality is improved with five level output and balanced active power sharing between the sources are achieved and also the bidirectional power flow has been archived. The two-stage SVPS extracts the maximum power from the solar panels from Incremental Conductance (IC) and Perturb and Observe (P&O) algorithms-based control of the DC-DC Converter. In this work, a single phase 2kW, 230-volt 5 level reduced switch count/Asymmetrical multi-level inverter has been designed for the Domestic as well as for the grid integration applications and its performance parameters like THD, Voltage regulation, reactive power support, total power loss and efficiency are discussed for both the control algorithms as mentioned above. The Simulation of this system is implemented on MATLAB/SIMULINK Software and the Comparative study for parameters involved in power quality improvement are carried out.

IndexTerms **- Cascaded H-Bridge multi-level inverter, Maximum power point tracking, Power quality, PPCS.**

I. INTRODUCTION

Photovoltaic power conversion system (PPCS) usually requires a DC-DC Converters and Inverters as Power electronic interface between the solar panel input and the load. In general, the two-level inverters and multi-level inverters are used. Due to lower switching stresses, lower operating frequency and smaller filter requirements makes multi-level inverters. There are number of advancements are taking place in the multi-level inverters and advance topologies are reported which uses lesser advance topologies are reported which uses lesser switches, has a greater number of steps and lower THD values.

An E-type inverter using current control technique is described in [1]. This configuration has good reliability and the output is power factor corrected, modified T-type inverter with reduced zero state conduction losses has been described in [2]. It uses direct power control to achieve faster dynamic response balanced neutral point and controlled power output. Single sourced DC converter having multiple output ports are used in cascaded H-Bridge inverters where there is need for multiple sources such as efficient asymmetrical Cascaded H-Bridge multilevel inverters for single stage photovoltaic PV is described in [3].

A transformer less compact topology is presented in [4]. But without transformer, the DC currents get injected into the grid causing a saturation problem in the distribution transformers. In present days cascaded multi-level inverter topologies are predominantly used but they require separate DC supplies. Since the onset of solar energy conversion systems, the number of DC inputs need not to reduce as such any number of DC voltages might be achieved from a solar panel by using a single converter is explained in [5]. It uses a toroidal core which provides a galvanic isolation between input and output sides of the converter. In [6] a control method is given for selective harmonic elimination. This is achieved by converting the nonlinear equations to a specific control system using look up tables and an integral controller which converges the system to a steady state with zero error. The calculations get simplified but the procedure is tedious.

Temperature dependency and distinct irradiations can lead to panel mismatch in PPCS. A control scheme presented in [7] balances the DC link capacitors in every H-Bridge of the system even during power mismatch in PPCS. The topology helps improve the utilization of connected PV panels that are individually connected to each DC link. Multi-level inverters are becoming more and more popular in medium and high-power applications [8]. This is due to several inherent advantages of multi-level inverters over two-level inverters such as high-quality output, lower device ratings and several others. Maximum power point needs to be tracked in order to utilize the solar panels at their maximum efficiency at a given irradiation [9]-[11]. There are several common algorithms some of them are being the Incremental Conductance and Perturb and Observe.

II. CIRCUIT CONFIGURATION

The inverters that are grid connected systems are used these days to improve power quality in the grid. The system or a new modification in the H-bridge was provided by M. S. B. Ranjana and et al in [12]. Basically, the components of the modified topology are five switches, a diode and two dc sources that are independent. Here, 5 level was achieved with just 5 switches and a diode

whereas the basic circuit takes at least 8 switches in order to accomplish 5 levels. The authors have tried to improve this circuit by removing the uncontrollable diode and replacing it with a switch, which is controllable to our advantage. Another upper hand of the topology proposed here is that it can be used for resistive as well as inductive loads. The circuit diagram is depicted in Fig. 1. The new MLI proposed is used for power quality applications intended for its use in rural areas. The increased levels help reduce the THD of the current waveforms, abiding by the IEEE-519 standard. The DC sources used, meant to be the isolated ones, are derived from the solar array simulator. Here equal voltages are applied as input. The voltage sources, both valued V1 volts are applied as input. The switches S1 to S6 are provided gate signals by Sinusoidal Pulse Width Modulation with Fundamental Switching Frequency. The output voltage levels are therefore obtained as: 2V1, V1, 0, −V1, −2V1.

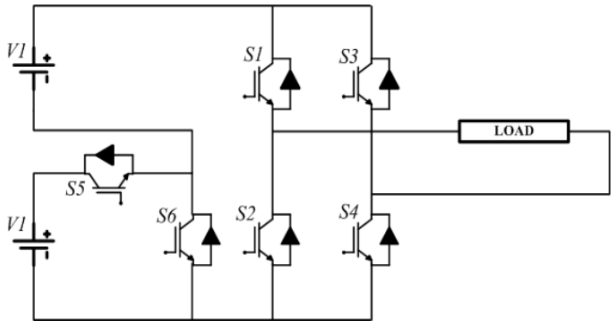

Fig. 1. Proposed five level multilevel inverter

Table I
State of Switches for Different Voltage Levels

Voltage Level	S1	S2	S3	S4	S5	S6
$+2V_1$	1	0	0	1	1	0
$+V_1$	1	0	0	1	0	1
0	1	0	1	0	0	0
$-V_1$	0	1	1	0	0	1
$-2V_1$	0	1	1	0	1	0

The proposed MLI topology is integrated into the power system as shown in Fig. 2. The multiple independent DC sources are obtained using a single input multiple output SEPIC converter as proposed in [13].

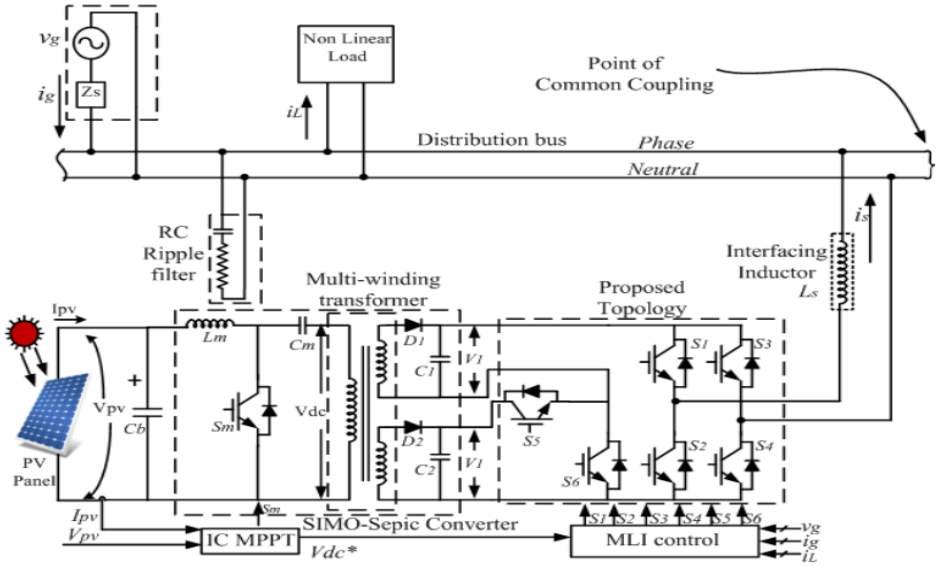

Fig. 2. Grid connected configuration of the proposed MLI

The control diagram for the grid integrated system is explained in Fig. 3. The grid voltage, grid current and the load current values are sensed. The second order generalized integral (SOGI) technique is achieved [14].

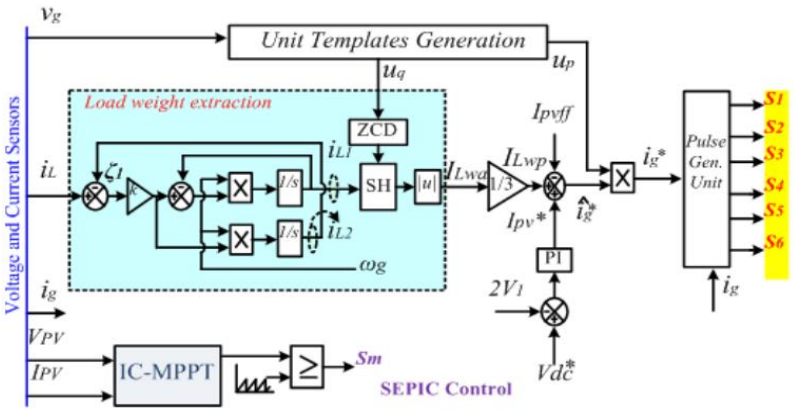

Fig. 3. Control layout of the proposed system for grid integration

III. MPPT ALGORITHMS

In a 24-h day, sunlight is only available for a limited time and depends heavily on weather conditions. In most photovoltaic power systems, a particular control algorithm, namely maximum power point tracking (MPPT), is utilized to take full advantage of the available solar energy. In this paper two different algorithms are explained in detail they are:

a) Incremental Conductance and
b) Perturb and Observe.

a). *Incremental Conductance Algorithm*

The incremental conductance algorithm is a Maximum Power Point Tracking (MPPT) algorithm used in photovoltaic (PV) systems. It's a popular algorithm because it's highly productive and has high tracking correctness in quickly changing atmospheric conditions.

The algorithm works by measuring the change in power with respect to the change in voltage and current at each step. Detecting the slope of the P–V curve. Searching the peak of the P–V curve. Tuning the duty cycle of the converter in fixed step size until the peak of the P–V curve is reached. The flowchart for implementation of the I&C algorithm is depicted in Fig. 4.

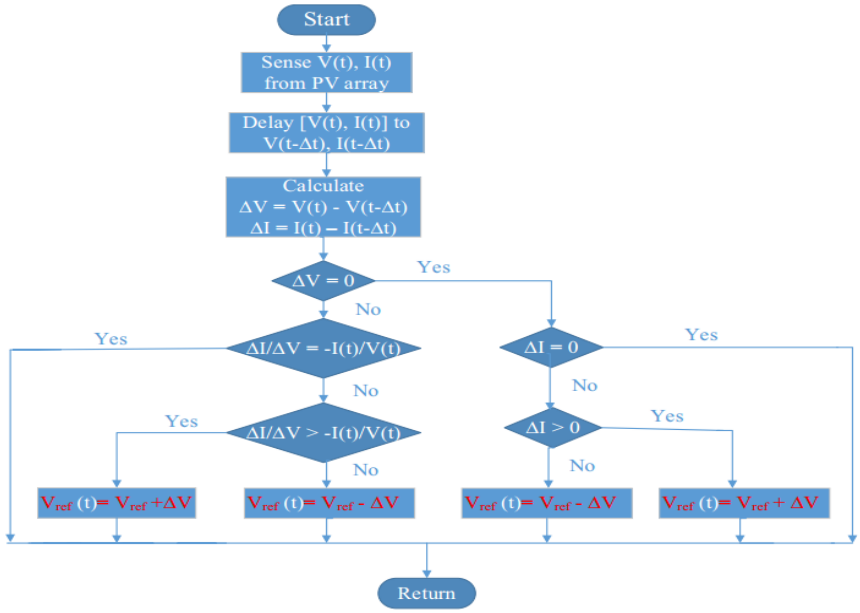

Fig. 4. Flowchart of Incremental Conductance Algorithm

b). *Perturb and Observe Algorithm*

The Perturb and Observe (P&O) algorithm is a commonly used Maximum Power Point Tracking (MPPT) algorithm for photovoltaic (PV) generators. The algorithm works by:

- Perturbing: Adding a small perturbation to the current set-point.
- Observing: Observing the impact on the output power.
- Comparing: Comparing the PV power output with the previous perturbation cycle.

Figure 5 depicts the flowchart for implementation of the P&O algorithm; first, the practical voltage and current from PV array are measured. After that, the product of voltage and current gives the actual power of PV module. Then, it will check status what whether ΔP = 0 or not. If this status is satisfied, then operating point is at the MPP. If it is not satisfying, then it will check another status that ΔP >0. If this status is satisfied, then it will check out that ΔV >0. If it is satisfied, then it indicates that operating point is at the left side of the MPP. If ΔV > 0 status is not satisfied, then it indicates that operating point is at the right side of the MPP. This process is continuously repeated until it reached the MPP. So, at all times there is a compromise between the increments and the sampling rate in the P&O algorithm.

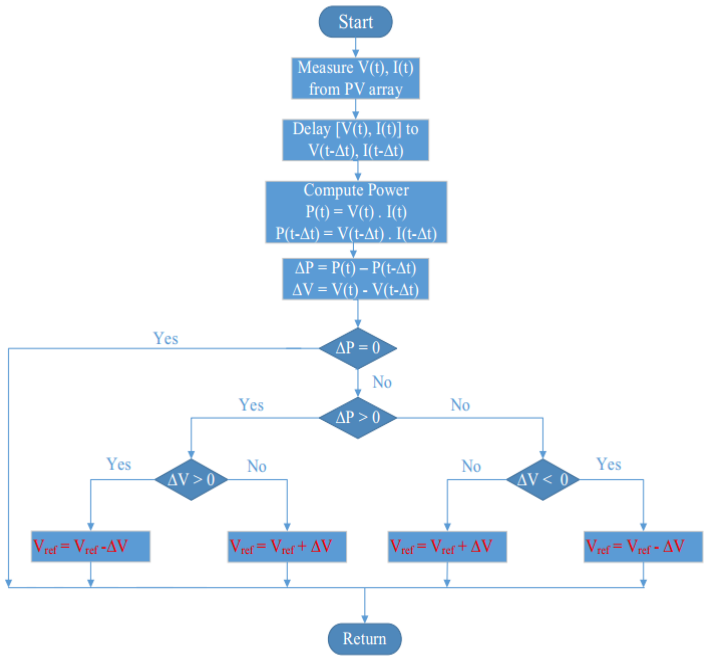

Fig. 5. Flowchart of Perturb and Observe Algorithm

IV. SEPIC Converter Design, Loss and Efficiency Calculation

A SEPIC converter is the single-ended primary inductance converter as shown in Fig. 6. The SEPIC can produce an output voltage that is either greater or less than the input but with no polarity reversal. To derive the relationship between input and output voltages, these initial assumptions are made:

1. Both inductors are very large and the currents in them are constant.
2. Both capacitors are very large and the voltages across them are constant.
3. The circuit is operating in the steady state, meaning that voltage and current waveforms are periodic.
4. For a duty ratio of D, the switch is closed for time DT and open for (1-D) T.
5. The switch and the diode are ideal.

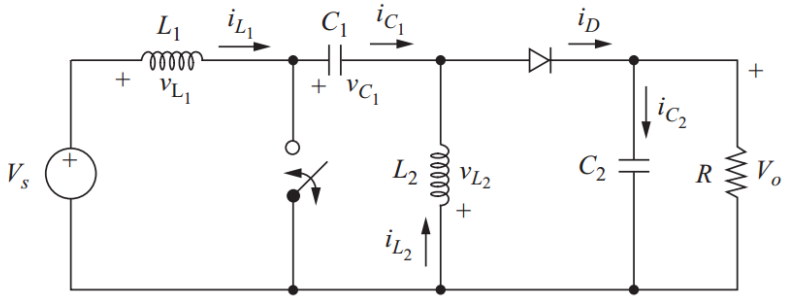

Fig. 6. SEPIC Converter

The inductor current and capacitor voltage restrictions will be removed later to investigate the fluctuations in currents and voltages. The inductor currents are assumed to be continuous in this analysis. Other observations are that the average inductor voltages are zero and that the average capacitor currents are zero for steady-state operation.

The SIMO-SEPIC Converter needs only one inductor and one Capacitor, the remaining components are replaced by the High Frequency Transformer. The values of Duty ratio (D), Primary Inductance (L_1), Primary Capacitance (C_1) are designed as detailed below.

$$D = \frac{v_0}{v_0 + v_S} \quad \ldots\ldots\ldots (1)$$

$$L_1 = \frac{v_S D}{\Delta i_{L_1} f} \quad \ldots\ldots\ldots (2)$$

$$C_1 = \frac{v_0 D}{R f \Delta v_{C_1}} \quad \ldots\ldots\ldots (3)$$

Where,

V_s = Input Voltage, V_0= Output Voltage, Δi_{L_1} = Change in Inductor Current, Δv_{C_1} = Change in Capacitor Voltage, f = Switching Frequency, R = Load Resistance.

The efficiency calculation could be done using several approaches. The losses are calculated first and then deducted from the input power. This gives the output power and hence an easier and precise way to calculate the efficiency. Some of the data used for the prediction of efficiency are obtained from manufacturers data sheet of the switches. Some others are measured directly from the hardware set up using Fluke Scope meter. The total losses can be categorized into two: Conduction losses and switching losses. The conduction loss is calculated by the following relation:

$$Pc = Voc * Ioc * ton * \text{f1} \quad \ldots\ldots\ldots (4)$$

Where,

V_{oc} = Maximum forward drop of the Switch, (V)

I_{oc} = Maximum current through the switch, (A)

t_{on} = switch ON time, (s)

f_1 = fundamental frequency, (Hz)

The switching loss during the transit of states is found using the equation:

$$P_w = \frac{v_d * I_d * (t_{con} + tc_{0ff}) * fs}{2} \quad \ldots\ldots\ldots (5)$$

Here

$$t_{con} = t_{don} + t_r + t_f \quad \ldots\ldots\ldots (6)$$

$$t_{coff} = t_{dof\,f} + t_r + t_f \quad \ldots\ldots\ldots (7)$$

Where, t_{con} - time for turning ON the switch, t_{don} - switch ON delay time, t_r - output voltage rise time, t_f - output voltage fall time, t_{coff} - time taken to turn OFF the switch, t_{doff} - delay time in turning OFF the switch, f_s - switching frequency

The total efficiency derived from basic formula:

$$\eta = \frac{P_{in} - P_T}{P_{in}} \quad \ldots\ldots\ldots\ldots (8)$$

P_{in} is the DC input power and P_T is the total losses

The efficiency calculation is evaluated. The data used for the prediction of efficiency are obtained from manufacturer Technical data sheet of the IGBT power switch IXYH82N120C3 [15]. t_{don}= 29ns, t_{doff} = 280ns, t_f = 93ns with V_{GE} = 15V and R_G = 2Ω.

V. SIMULATION STUDIES

The Simulation of five level inverter is carried out in this section, here the simulation is done using MATLAB/SIMULINK model. The two types of algorithmic techniques are used to track the solar panel output as discussed in the above. The PWM technique used here to provide logic signals for the IGBT Switches is SPWM with fundamental switching frequency. The simulation studies are carried out two variations performing at the grid side are discussed in this section.

a) THE INVERTER OUTPUT IS CONNECTED TO THE LOAD OF 1KW AND REMAINING POWER WILL BE RECEIVED BY THE GRID.

b) THE INVERTER OUT IS CONNECTED TO THE PRACTICAL GRID CONSIDERING THE TRANSFORMER, TRANSMISSION LINE AND A LOAD OF 1KW IS CONNECTED PARALLEL TO IT.

5.1 The Inverter output is connected to the load of 1KW and remaining power will be received by the grid using I and C Algorithm

The simulation of Incremental Conductance algorithm is shown in fig 7. The input parameters from the solar panel is fed to the SIMO-SEPIC Converter as shown in Fig. 8. The design of SEPIC Converter in such a way that the output voltage of 325V (P-P) and 8A Current is divided into the two sources using the multiple output Transformer to provide the source for the 5-Level inverter. The grid active power is negative as it draws active power from the PV. The MLI injects active power into the point of common coupling (PCC) and thus supports the load is completely compensated by the MLI since the reactive power demand of the load is equal to that of the MLI.

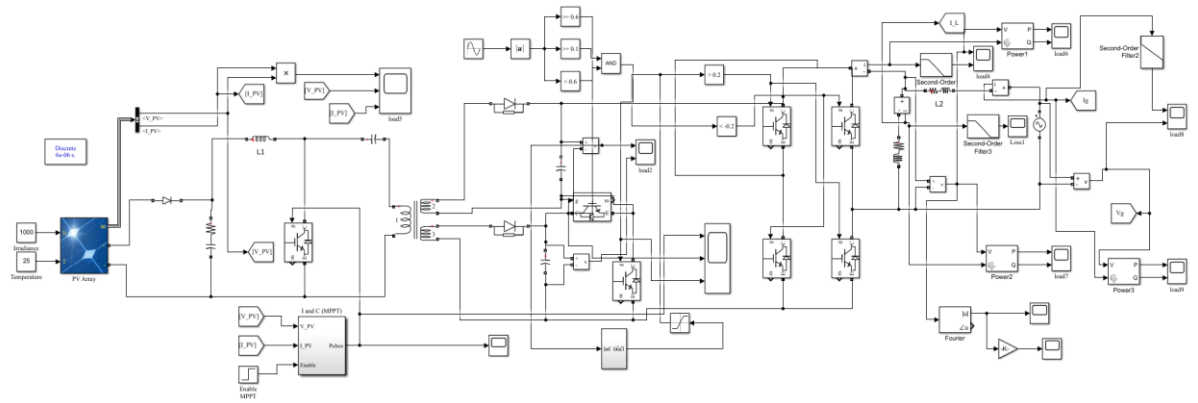

Figure 7 Simulation Diagram with I & C Algorithm

The test results of the grid connected MLI operation is depicted in Fig. 9. The grid voltage and current are sinusoidal and in phase. The THD after reactive power injection is tabulated with respect to both the Algorithms. The THD spectra of grid current, voltage, the load current, voltage, the inverter current and voltage are shown in Fig. 10. The grid voltage is devoid of any harmonics even after the grid integration. The harmonics in the load current are completely compensated and a sinusoidal, in-phase grid current is obtained by the proposed system operation.

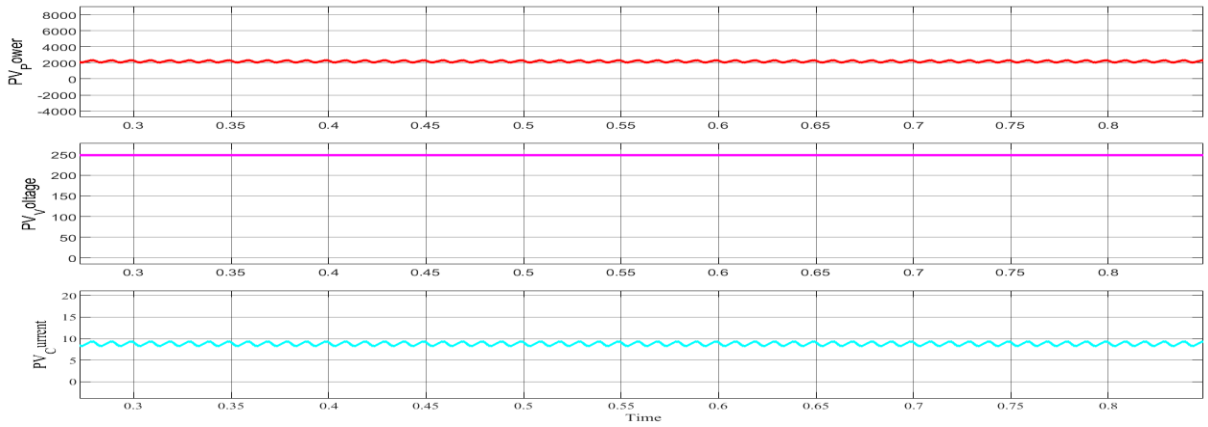

Fig 8 Solar PV input parameters

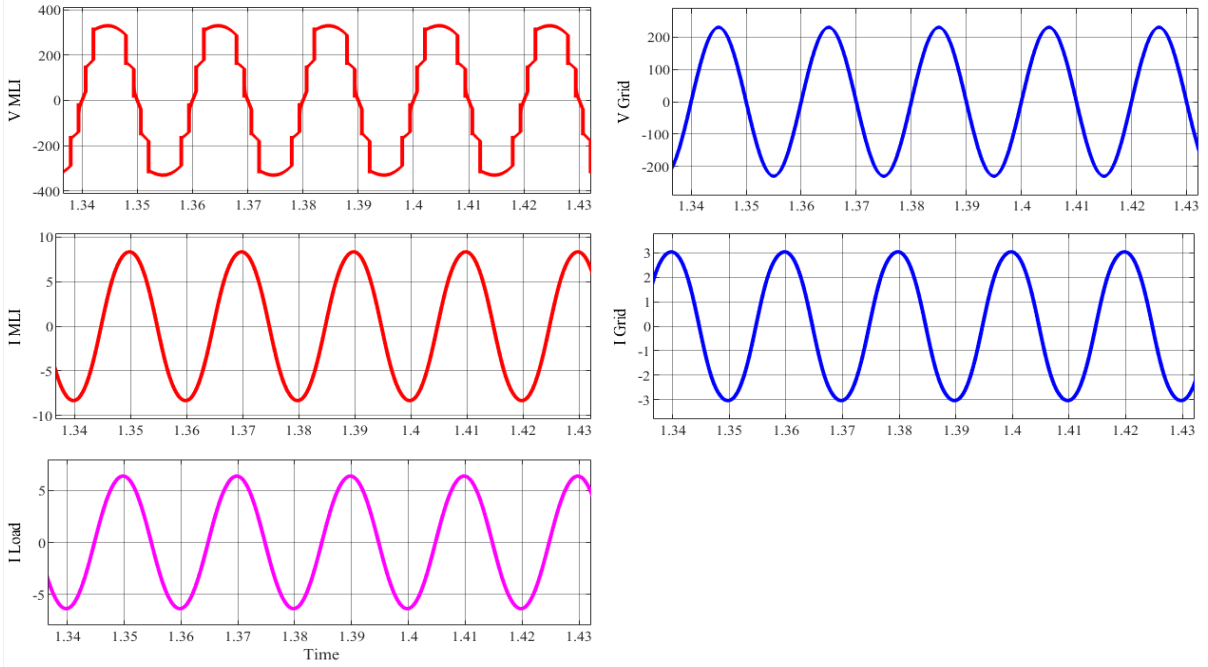

Fig. 9 Performance results of proposed system using I & C Algorithm

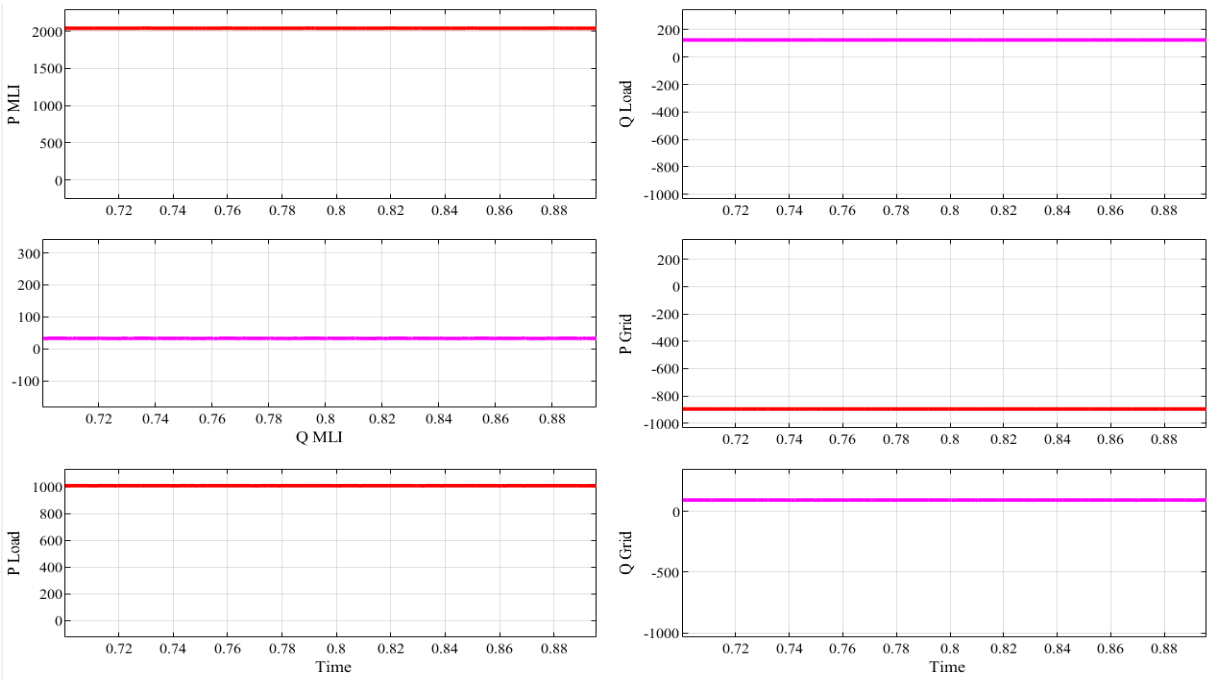

Fig. 10 Active and reactive power sharing in I & C Algorithm

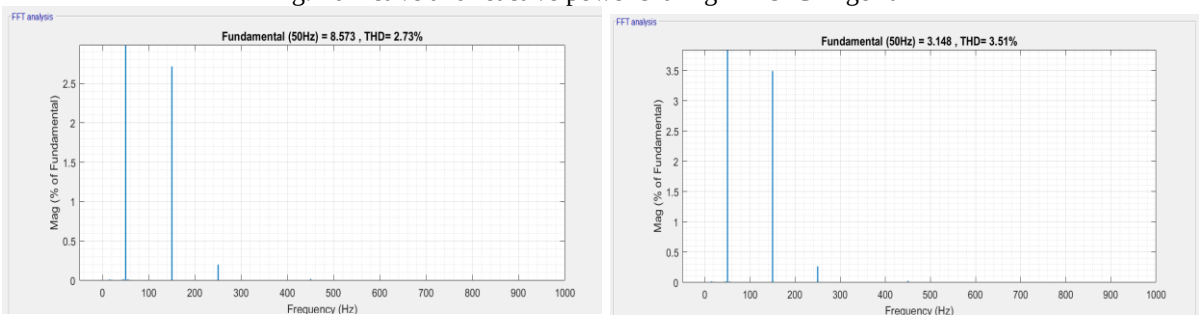

(a) (b)

Fig. 11 current THD% of the (a) Inverter and (b) Grid

The THD analysis of the inverter, load and grid using Incremental conductance MPPT Algorithm of both R and RL Load are discussed below. The current THD of proposed system limits with in the IEEE Standard. The current THD values are shown in fig 11. The voltage THD of the proposed system is shown in fig 12.

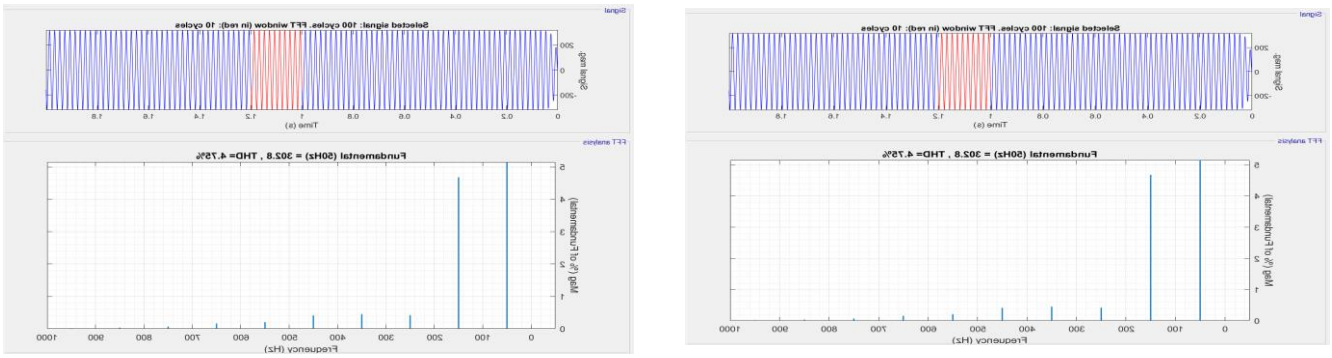

(a) (b)

Figure 12 Voltage %THD values of (a) Inverter and (b) Load

5.2 The Inverter output is connected to the practical grid considering the transformer, transmission line and a load of 1KW is connected parallel to it using I and C Algorithm.

The Simulation in this Set of variation, a practical grid parameter is considered such as transformer and transmission line after that it is connected to the grid. In parallel to the grid standard 1KW of load is connected as shown in the simulation diagram of figure 13. The transformer taken as linear transformer and the transmission line considered for the transmission of power from the inverter to grid.

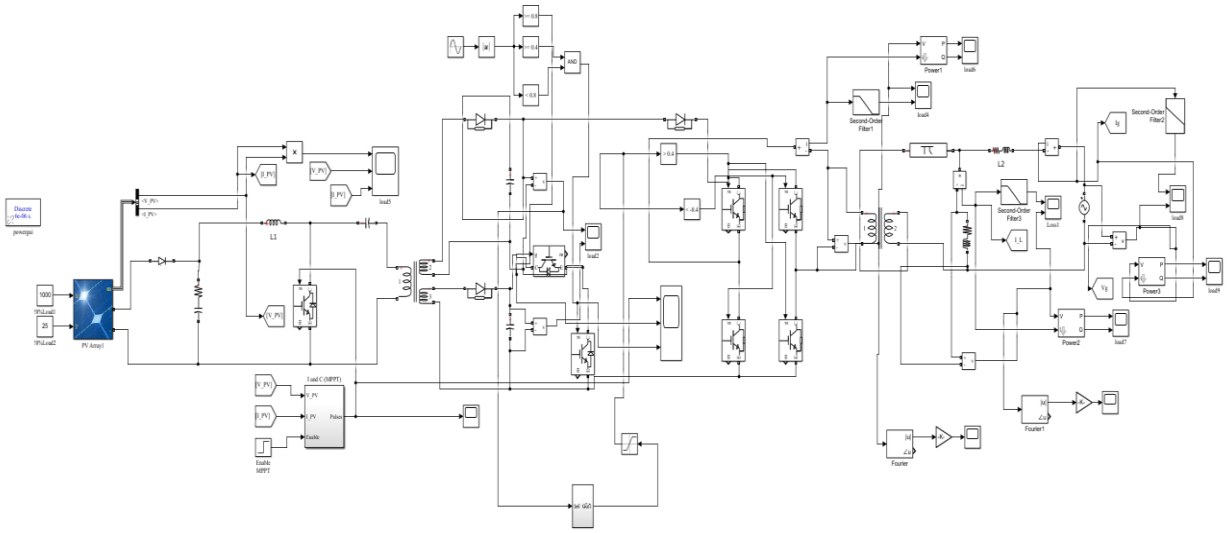

Figure 13. Simulation diagram of the proposed system

The transmission line contains the standard parameters like frequency of the used RLC specification and resistance, inductance and capacitance per unit length of the transmission line as shown in the block parameters. The performance results are appropriately equal to the first variation as discussed in the above simulation waveforms. The performance parameters including THD, rms voltage, power loss, voltage regulation and efficiency are discussed in the further section in the results discussion. The simulation results and electrical parameters with respect to both the algorithms are discussed.

5.3 The Inverter output is connected to the load of 1KW and remaining power will be received by the grid using P and O Algorithm

The Simulation diagram with respect to the P & O Algorithm technique is shown in figure 14.

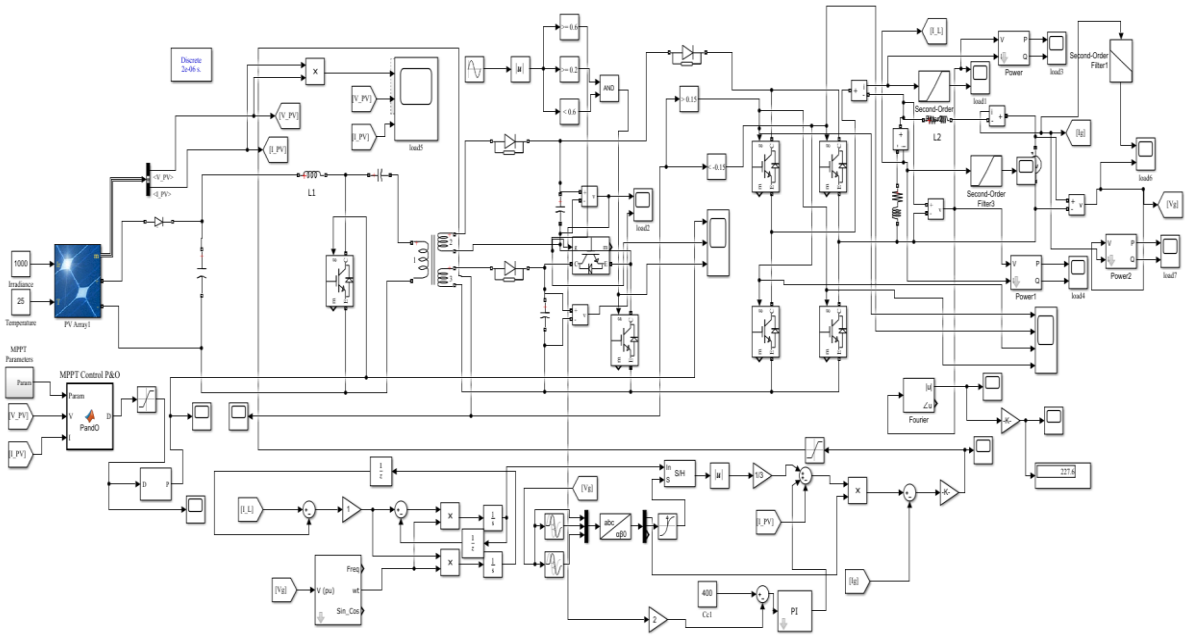

Figure 14 Simulation diagram of P & O Algorithm Technique

The solar PV input parameters remains approximately same for both the Algorithmic Techniques. The performance results of the proposed system is shown in fig. 15. The active and reactive power sharing between inverter, load and grid as shown in fig. 16. The current THD values of inverter load and grid for both R and RL Load are tabulated in next section and are shown in fig. 17. The voltage THD values of the inverter is shown in fig. 18.

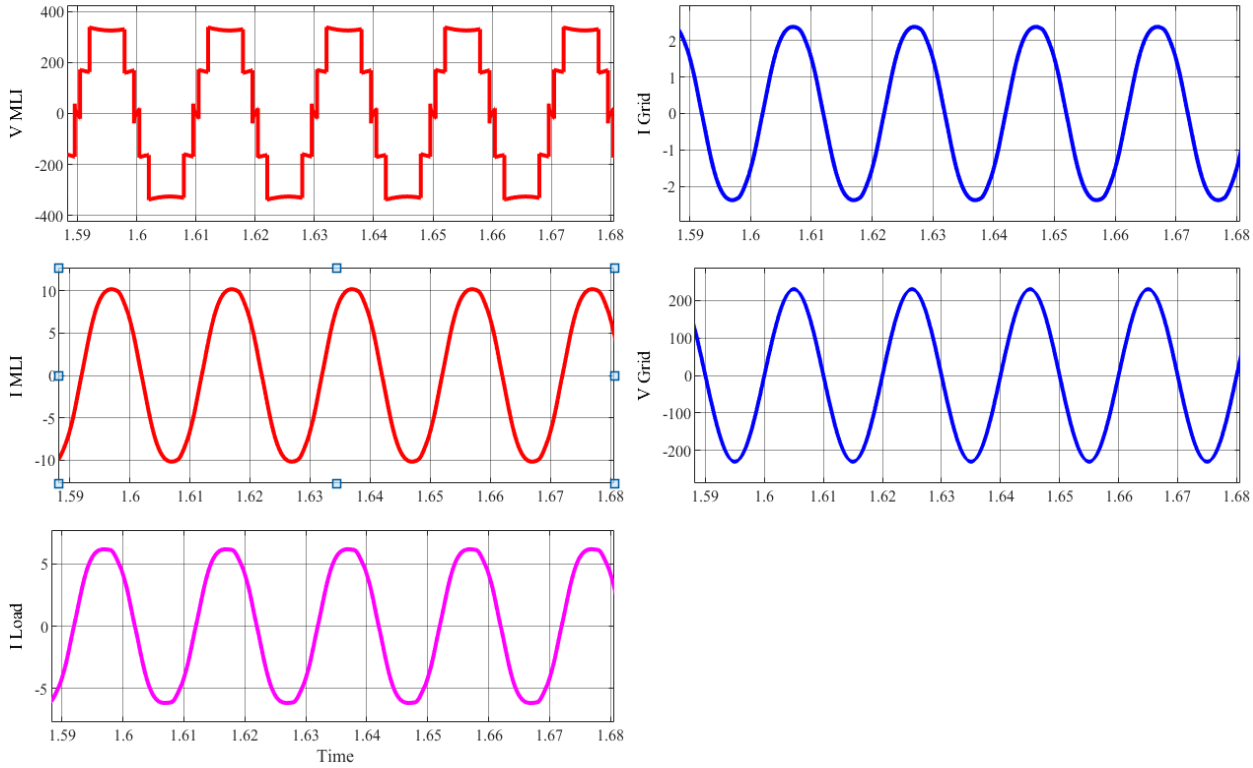

Fig 15 Performance results of the proposed system using P & O Algorithm

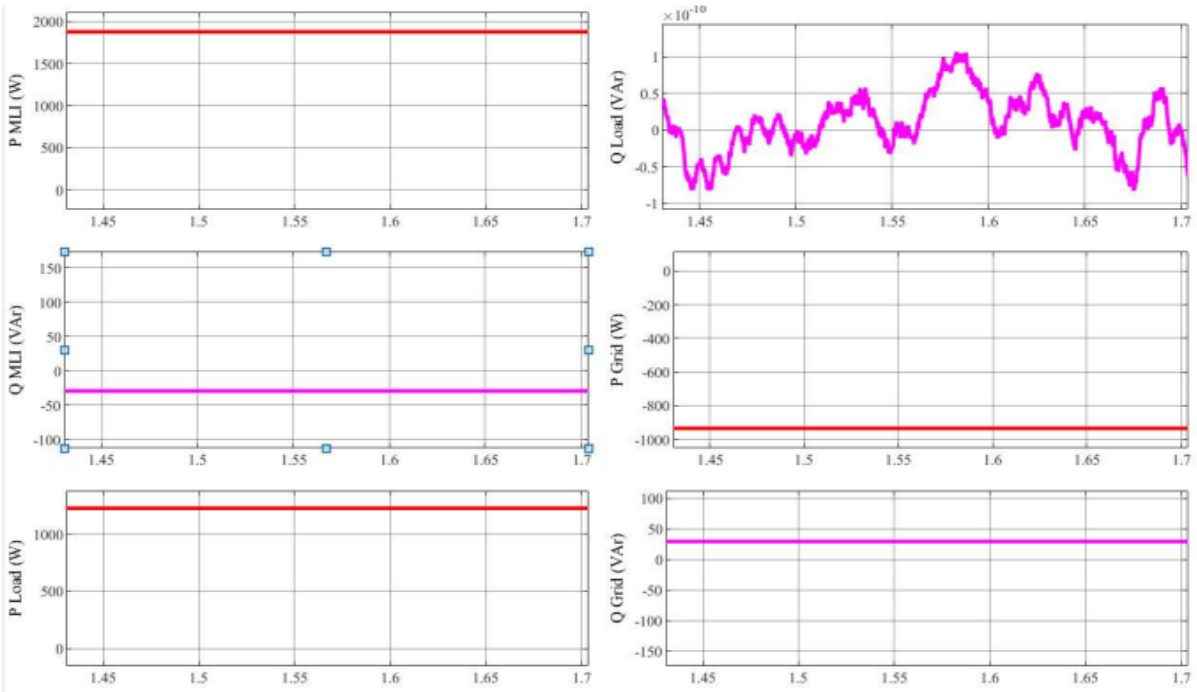

Fig 16. Active and reactive power sharing in P & O Algorithm technique

The THD values of the Inverter, load and grid are analyzed in both algorithmic techniques and the results are tabulated in the results discussion. The figure 16 and figure 17 shows the THD values of the inverter, load ang grid.

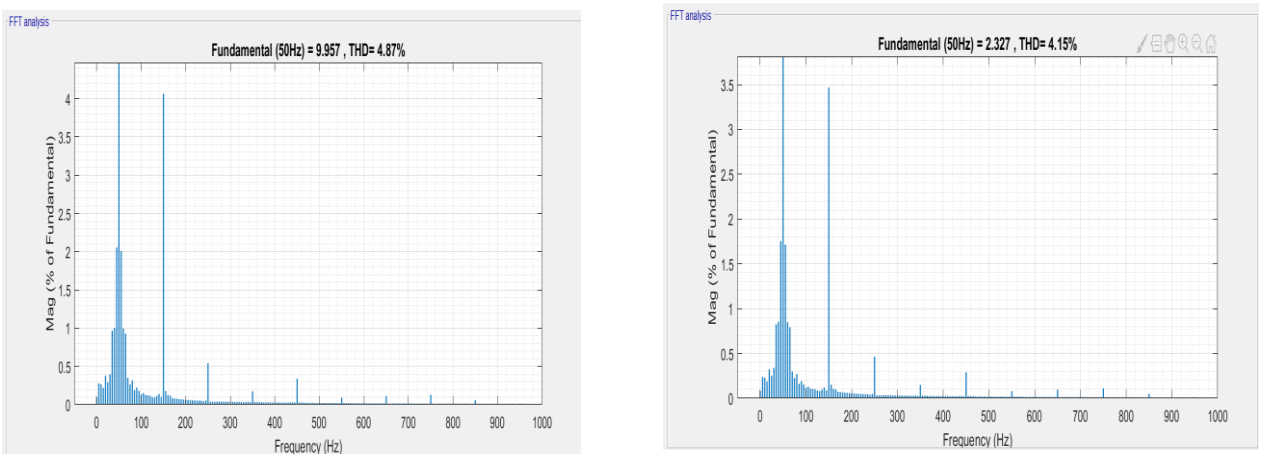

(a) (b)

Fig. 17 current THD values of RL Load (a) Inverter and (b) Grid

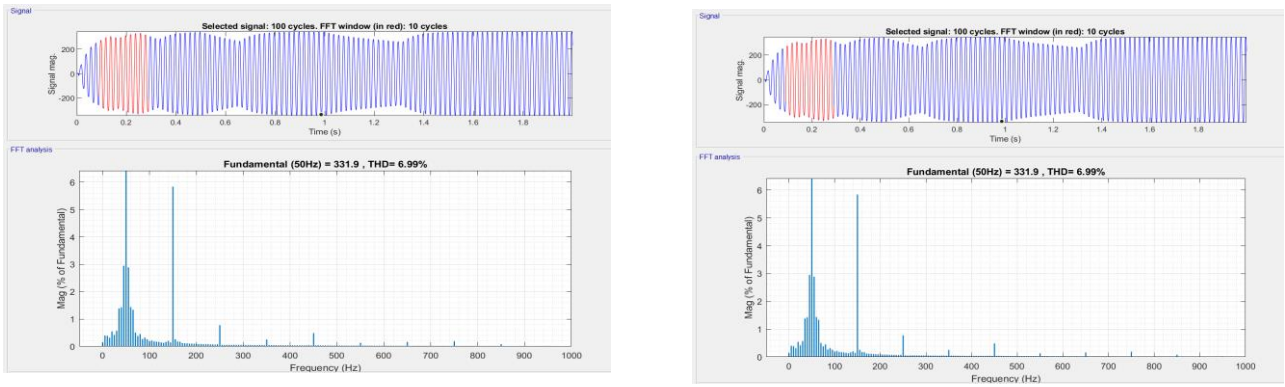

(a) (b)

Figure 18 Voltage %THD values of (a) Inverter and (b) Load

5.4 The Inverter output is connected to the practical grid considering the transformer, transmission line and a load of 1KW is connected parallel to it using I and C Algorithm.

The Simulation in this Set of variation, a practical grid parameter is considered such as transformer and transmission line after that it is connected to the grid. In parallel to the grid standard 1KW of load is connected as shown in the simulation diagram 19. The transformer taken as linear transformer and the transmission line considered for the transmission of power from the inverter to grid.

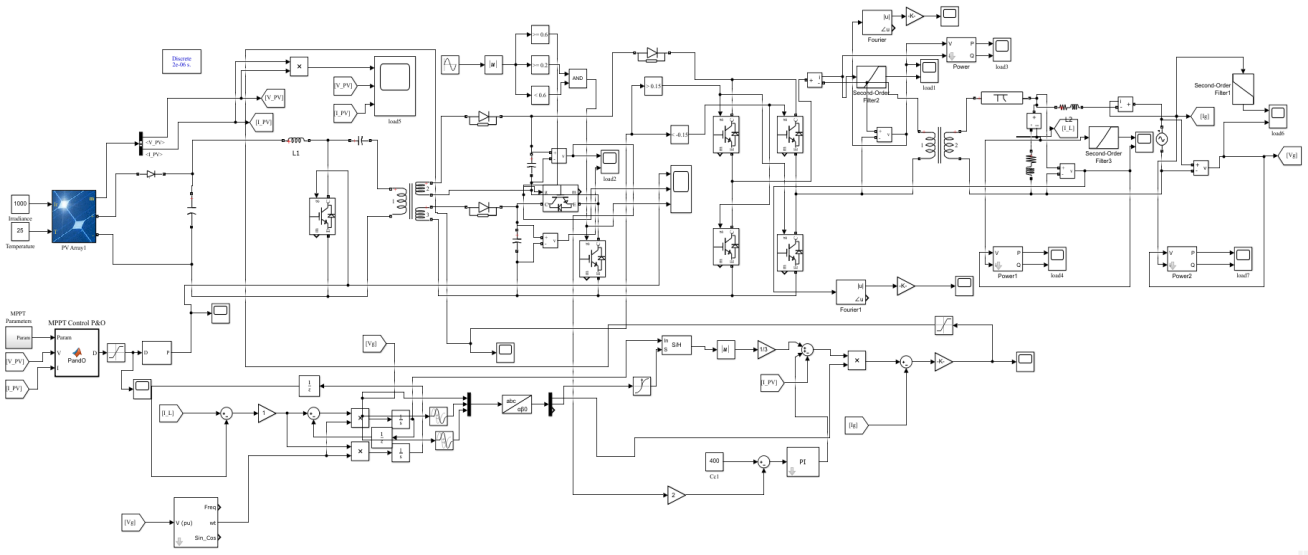

Figure 19 Simulation diagram of P & O Algorithm Technique

The transmission line contains the standard parameters like frequency of the used RLC specification and resistance, inductance and capacitance per unit length of the transmission line as shown in the block parameters. The performance results are appropriately equal to

the first variation as discussed in the above simulation waveforms. The performance parameters including THD, rms voltage, power loss, voltage regulation and efficiency are discussed in the further section in the results discussion. The simulation results and electrical parameters with respect to both the algorithms are discussed.

VI. RESULTS AND DISCUSSION

6.1 Results of 5-Level Inverter compared with both the algorithms.

a). The Inverter output is connected to the practical grid considering the transformer, transmission line and a load of 1KW is connected parallel to it

The simulation results of 5-level multilevel inverter with Incremental Conductance and Perturb and Observe Algorithm techniques for both Rand RL loads have been shown in this section. Here RMS output voltage, load current, % THD values, input power, output power has been measured directly on SIMULINK and total power losses and efficiency are calculated based on the simulation data. Analysis of THD and efficiency of 5-level multilevel inverter are discussed in design aspects section and simulation results have been discussed. Table 2 shows the THD analysis of 5-level multilevel inverter. Table 3 gives the Efficiency, power loss and RMS Voltage and voltage regulation values for both R and RL Load. The results are compared with both the algorithmic techniques are tabulated below.

TABLE 2 % THD VALUES OF 5-LEVEL INVERTER

Parameter	Load	I and C Algorithm			P and O Algorithm		
		Inverter	Load	Grid	Inverter	Load	Grid
Voltage %THD	R= 52.9Ω	4.9	4.9	0.05	6.99	6.99	0.03
	R= 52.9Ω L=5.36mH	4.75	4.75	0.05	6.6	6.6	0.03
Current %THD	R= 52.9Ω	4.22	3.26	4.74	3.31	4.76	4.15
	R= 52.9Ω L=5.36mH	3.85	1.5	2.22	3.3	4.77	4.1

The efficiency, Power loss, RMS voltage and Voltage Regulation of the 5-Level inverter with both the Algorithmic techniques are tabulated below.

Table 3 Comparison of efficiency, PL and V_{RMS} Voltage and Voltage Regulation

Parameters	I & C Algorithm		P & 0 Algorithm	
	R	RL	R	RL
Efficiency (%)	95.63	95.61	94.85	94.9
Power loss (W)	87.3	87.6	103	102
RMS Voltage (V)	229	228.2	226.5	226.8
Voltage Regulation (%)	0.4	0.7	1.5	1.3

b). The inverter output is connected to the practical grid considering the transformer, transmission line and a load of 1KW is connected parallel to it.

The simulation results in the second variation of the Simulink model for 5-Level inverter as been discussed here. Table 4 shows the voltage and current THD values inverter, load and grid with respect to both the algorithms. The remaining electrical parameters are remains approximately same as that of before results shown in Table 3.

Table 4 % THD values of 5-Level Inverter using Transmission line

Parameter	Load	I and C Algorithm			P and O Algorithm		
		Inverter	Load	Grid	Inverter	Load	Grid
Voltage %THD	R= 52.9Ω	5.78	5.74	0.04	8.59	8.6	0.02
	R= 52.9Ω L=5.36mH	5.78	5.74	0.05	8.47	8.48	0.02
Current %THD	R= 52.9Ω	3.84	2.23	1.49	3.31	4.76	4.15
	R= 52.9Ω L=5.36mH	3.84	2.23	1.47	3.3	4.78	4.1

VII. CONCLUSION

A new five-level inverter-based grid-connected photovoltaic power conversion system is proposed in this paper. The new topology is a modified H-bridge configuration where the minimum number of components are used for the five-level output w.r.t the reported topologies. The maximum power extraction from the PV panels is achieved by both IC and P & O based MPPT operation. From comparative study, it can be said that the 5-level multilevel inverter with Incremental Conductance technique has better performance compared to Perturb and Observe Algorithmic technique in considered various performance parameters except total Harmonic Distortion (THD) parameter. But, as THD of the Inverter, load and grid are within the limits of IEEE standard 519-2014, we can choose Incremental Conductance Algorithm control technique over Perturb and Observe Algorithm control technique as power losses are less in inverter with Incremental Conductance Algorithm control technique. The 5-level inverter topology is presented in this work requires less power electronic components and has high efficiency.

REFERENCES

[1] Marco di Benedetto, A. Lidozzi, F. Crescimbini and P. J. Grbovic, “Five-Level E-Type Inverter for Grid-Connected Applications,” IEEE Tran. On Ind. Ap., vol. 54, no. 5, Sept. 2018 pp. 5536-5548.
[2] G. Yang, S. Hao, C. Fu and Z. Chen, “Model Predictive DPC Based on Improved T-Type Grid-Connected Inverter,” IEEE Jour. of Emerg. And Selected Topics in Power Electron., vol. 7, no. 1, Mar 2019 pp. 252-260.
[3] Ahmed, M. S. Manoharan, and J.-H. Park, ‘‘An efficient single-sourced asymmetrical cascaded multilevel inverter with reduced leakage current suitable for single-stage PV systems,’’ IEEE Trans. Energy Convers., vol. 34, no. 1, pp. 211–220, Mar. 2019, doi: 10.1109/TEC.2018.2874076.
[4] Roberto Gonzlez, Eugenio Guba, Jess Lpez and Luis Marroyo, “Transformer less Single-Phase Multilevel-Based PV Inverter,” IEEE Tran. On Ind. Electron., vol. 55, no. 7, July 2008, pp. 2694-2702.
[5] M. M. Hasan, A. A. Siada, S. M. Islam, and M. S. A. Dahidah, “A New Cascaded Multilevel Inverter Topology with Galvanic Isolation,” IEEE Tran. on Ind. Ap., vol. 54, no. 4, Jul 2018 pp. 3463-3472.
[6] B. Sharma and J. Nakka, “Single-phase cascaded multilevel inverter topology addressed with the problem of unequal photovoltaic power distribution in isolated dc links,” IET Power Electron., Feb 2019, Vol. 12 Iss. 2, pp. 284-294.
[7] Hui Zhao, Tian Jin, Shuo Wang and Liang Sun, “A Real-Time SHE Based on a Transient-Free Inner Closed-Loop Control for Cascaded Multilevel Inverters,” IEEE Tran. on Power Electron., vol. 31, no. 2, Feb 2016 pp. 1000-1014.
[8] P. Omer, J. Kumar, and B. S. Surjan, ‘‘A review on reduced switch count multilevel inverter topologies,’’ IEEE Access, vol. 8, pp. 22281–22302, Jan. 2020, doi: 10.1109/ACCESS.2020.2969551.
[9] Xiao. W., Ozog. N., Dunford. W. G., “Topology study of PV interface for maximum power point tracking,” IEEE Trans. Ind. Electron., Apr 2007, 54,(3), pp. 1696-1704.
[10] Sukanya, C. M. Nirmal Mukundan, P. Jayaprakash, O. V. Asokan “A new topology of multilevel inverter with reduced number of switches and increased efficiency,” 2018 IEEE Int Conf on Power Electronics Drives and Energy Systems (PEDES), Dec 2018, pp. 1-6.
[11] Singaravel, M.M.R., Daniel, S.A., “MPPT with single DC-DC converter and inverter for grid-connected hybrid wind-driven PMSG-PV system,” IEEE Tran. Ind. Electron., Feb 2015, pp. 4849-4857.
[12] M. S. B. Ranjana, P. S. Wankhade, and N. D. Gondhalekar, “A modified cascaded H-bridge multilevel inverter for solar applications,” 2014 Int. Conf. on Green Computing Comm. and Elect. Eng., Coimbatore, Mar 2014, pp. 17.
[13] C. M. Nirmal Mukundan and P. Jayaprakash, “Solar PV fed cascaded H-bridge multilevel inverter and SIMO-SEPIC based MPPT controller for 3-phase grid connected system with power quality improvement,” 2017 Nat. Power Electron. Conf. (NPEC), Pune, Dec 2017, pp. 106-111.
[14] F. Xiao, L. Dong, L. Li and X. Liao, “A Frequency-fixed SOGI-Based PLL for Single-Phase Grid-Connected Converters,” IEEE Tran. on Power Electron., vol. 32, no. 3, Mar 2017, pp. 1713-1719.
[15] Littelfuse Discrete IGBT Datasheet IXYH82N120C3.